Journal of Archaeological Science: Reports 57 (2024) 104601

Contents lists available at ScienceDirect

Journal of Archaeological Science: Reports

journal homepage: www.elsevier.com/locate/jasrep

Burial of two closely related infants under a "dragon stone" from prehistoric Armenia

Arsen Bobokhyan [a,e,*], Miren Iraeta-Orbegozo [b,c,+], Hugh McColl [d], Ruzan Mkrtchyan [e], Hasmik Simonyan [a], Jazmín Ramos-Madrigal [f], Aída Andrades-Valtueña [g], Pavol Hnila [h], Alessandra Gilibert [i], Ashot Margaryan [d,f,j]

[a] Institute of Archaeology and Ethnography, National Academy of Sciences, Charents St. 15, 0025, Yerevan, Armenia
[b] Section for Molecular Ecology and Evolution, Globe Institute, Faculty of Health and Medical Sciences University of Copenhagen, 1353 Copenhagen K, Denmark
[c] School of Archaeology, University College Dublin, Belfield, Dublin 4, Ireland
[d] Lundbeck Foundation GeoGenetics Center, Globe Institute, Universiy of Copenhagen, Copenhagen, Denmark
[e] Yerevan State University, Alek Manukyan 1, 0025 Yerevan, Armenia
[f] Center for Evolutionary Hologenomics, Globe Institute, University of Copenhagen, Copenhagen, Denmark
[g] Department of Archaeogenetics, Max Planck Institute for Evolutionary Anthropology, 04103 Leipzig, Germany
[h] Freie Universität Berlin, Fachbereich Geschichts- und Kulturwissenschaften, Institut für Altorientalistik, Fabeckstraße 23-25, 14195 Berlin, Germany
[i] Ca' Foscari University of Venice, Dipartimento di Studi Umanistici, Dorsoduro 3484/D, 30123, Venice, Italy
[j] Institute of Molecular Biology, National Academy of Sciences, Hasratian St. 7, 0014 Yerevan, Armenia

ARTICLE INFO

Keywords:
Armenia
Caucasus
Bronze Age
Ancient DNA
Burial practices
Next-generation sequencing

ABSTRACT

"Dragon stones" are prehistoric basalt stelae carved with animal imagery found in Armenia and surrounding regions. These monuments have a complex history of use and reuse across millennia, and the original date of creation is still a matter of debate. In this article, we present a unique dragon stone context excavated at the site of Lchashen, Armenia, where a three-and-a-half-meter high basalt stela with an image of a sacrificed bovid was found above a burial dating to the 16th century BC. The burial stands out among hundreds from this site as the only one in connection with a "dragon stone", and one of very few containing the remains of newborn babies. Furthermore, our analyses of ancient DNA extracted from the well-preserved skeletal remains of two 0–2-month-old individuals showed them to be second-degree related females with identical mitochondrial sequences of the haplogroup U5a1a1 lineage, thus indicating that the infants are closely related. Additionally, we assessed that the buried individuals displayed genetic ancestry profiles similar to other Bronze Age individuals from the region.

1. Introduction

"Dragon stones" (Arm. *Vishapakar*) are ca. 150–550 cm high stelae of basalt carved with animal imagery and found in mountain meadows of present-day Armenia and neighboring regions (modern Southern Georgia and Eastern Turkey) (Fig. 1). Their current vernacular name likely connects to local folk tales of dragons in the shapes of mythical bulls, fish and snakes living in the mountains, as divine guardians of water and thunder. Until now, ca. 150 known examples of dragon stones have been recorded, which are usually found collapsed to the ground at secluded, water-rich meadows located between 2000 and 3000 m above sea level. From their shape and iconography, previous research (Gilibert et al., 2012) identified three main classes of dragon stones: *piscis* (fish-shaped), *vellus* (carved as if the hide of a bovid had been draped on them), and *hybrid* (combining the iconographies of both types). Based on the ongoing excavations at the site of Karmir Sar on Mount Aragats (N 40.418336°, E 044.145849°, 2850 m above sea level) (Hnila et al., 2019), we favor the interpretation of dragon stones as commemorative monuments located in the centers of open-air sanctuaries. At Karmir Sar, the earliest known dragon stones were erected at the end of the fifth

* Corresponding author.
E-mail addresses: arsen.bobokhyan@sci.am (A. Bobokhyan), orbegozo@sund.ku.dk (M. Iraeta-Orbegozo), hugh.mccoll@sund.ku.dk (H. McColl), ruzantrop55@mail.ru (R. Mkrtchyan), hassimonyan89@gmail.com (H. Simonyan), jazmin.madrigal@sund.ku.dk (J. Ramos-Madrigal), aida_andrades@eva.mpg.de (A. Andrades-Valtueña), pavol.hnila@fu-berlin.de (P. Hnila), alessandra.gilibert@unive.it (A. Gilibert), ashotmarg2004@gmail.com (A. Margaryan).
+ Joint first author.

https://doi.org/10.1016/j.jasrep.2024.104601
Received 21 June 2023; Received in revised form 23 March 2024; Accepted 14 May 2024
Available online 2 June 2024

millennium BC. Later, they were repeatedly re-embedded in various ritual and secular contexts. Whether these episodes of re-embedment went together with radical re-semantizations of the symbolic and mythological meanings of the steles or rather provided a long-term framework of survival and transmission of ancestral beliefs remains open to discussion. While early research on dragon stones concentrated mainly on the art-historical aspects of the phenomenon, more recent works apply the tools of modern archaeology and shift the accent to the surrounding landscape and archaeological context (cf. Gilibert et al., 2012; Bobokhyan et al., 2015; 2018; Hnila et al., 2019). The current article aims at advancing the discussion further by addressing the problem from a new perspective, implementing an interdisciplinary approach based on ancient DNA (aDNA) from two human remains excavated under one of such monuments in Lchashen, Armenia.

2. The Lchashen site and the dragon stone context

Lchashen is located on the north-western edge of the high-altitude Sevan Lake and is one of the most important archaeological site-clusters in Armenia (Fig. 2). Since 1950s, investigations of the site have expanded our understanding of the development patterns of the Bronze and Iron Age societies in South Caucasus. The site includes an Iron Age fortress with an Urartian cuneiform rock inscription of king Argishti I from the 8th century BC, an Early and Middle Bronze Age settlement within the area of the fortress, and Middle to Late Bronze Age cemeteries, including a cluster of separate elite barrows in the area of the modern Lchashen village. From the cuneiform inscription, we know the name of the fortress-town during the Iron Age, and possibly also earlier – Ishtikuni (for details cf. Petrosyan, 2018; 2022). Lchashen became well known in world archaeology especially due to finds of well-preserved wheeled wooden vehicles from the Late Bronze Age tombs, which emerged after the waters of Lake Sevan had decreased in level (Piggott, 1968).

The archaeological landscape of Lchashen includes two dragon stones, one of which is directly connected to this study (Khanzadyan, 2005; cf. Bobokhyan et al., 2017). It was discovered in 1980, 2.5 km south-west of the village Lchashen, in an ancient cemetery area called "Hamaliri taratsk" (Complex area, N 40.50779°, E 44.91174°, 1975 m above sea level), while installing water pipes. After being investigated in situ, the stela with materials found within the partly destructed burial, was transported to the Metsamor Historical-Archaeological Museum Reserve in the same year and placed at the museum's entrance (Figs. 1-6).

Although the machine excavator installing the water pipe dug over the barrow, it was still possible to investigate the context. According to the short preliminary report published by Khanzadyan (2005), the stela was found at a depth of 1.5 m below the surface, above a burial chamber identified at a depth of 2.5 m below the surface. The earthen barrow with pebble filling was surrounded by ca. 10 mid-sized circular stone barrows, which formed a cluster separate from the main Bronze Age cemeteries at Lchashen. The burial chamber was quadrangular and oriented from north to south (Fig. 3).

Khanzadyan reports broken artefacts, animal bones and incomplete human skeletal remains scattered all over the tomb (Figs. 4-5). She interpreted the disturbed find context as evidence for ancient looting and, based on the find position of the skull, she proposed to reconstruct the burial as the inhumation of an adult individual laid down on its left side in a hocker position. The materials found during the excavations include seven pottery vessels, a bronze hair ring, a carnelian bead, a bone needle and an obsidian tool (Fig. 4). The hair ring was found under the skull of an adult individual, a vessel with a stamped ornament was recorded adjacent to the back of the same individual. In the centre of the tomb, near a medium-sized rough stone, there were fragments of painted and simple-ware vessels, parts of a pot with finger imprints and a bead. In the south-western part of the tomb three simple pots were placed.

The dragon stone was found well-preserved above the burial chamber. The excavations could not determine whether this position had been the result of a collapse or rather an intentional setting. The stela is made

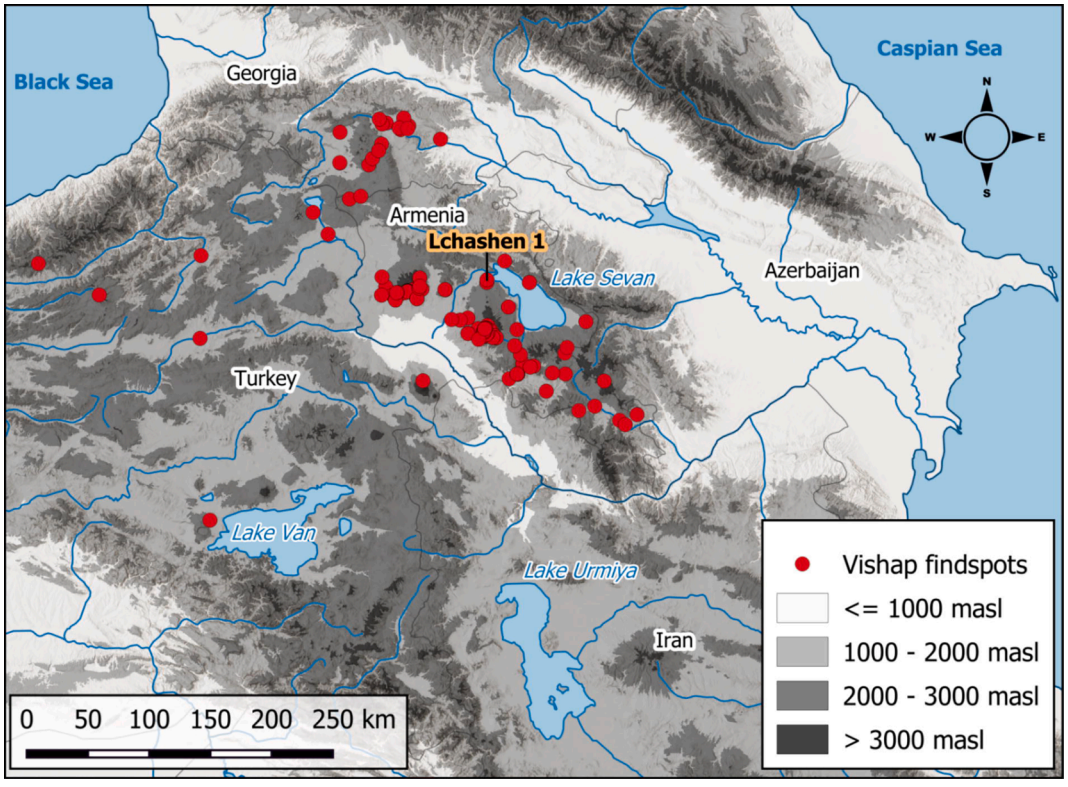

Fig. 1. Topographic map of the South Caucasus indicating the locations of dragon stone monuments (red circles) discovered so far; *P. Hnila, Catalogue: A. Bobokhyan/ A. Gilibert/P. Hnila, Topography: GMTED2010 and Natural Earth.* masl – meters above sea level.

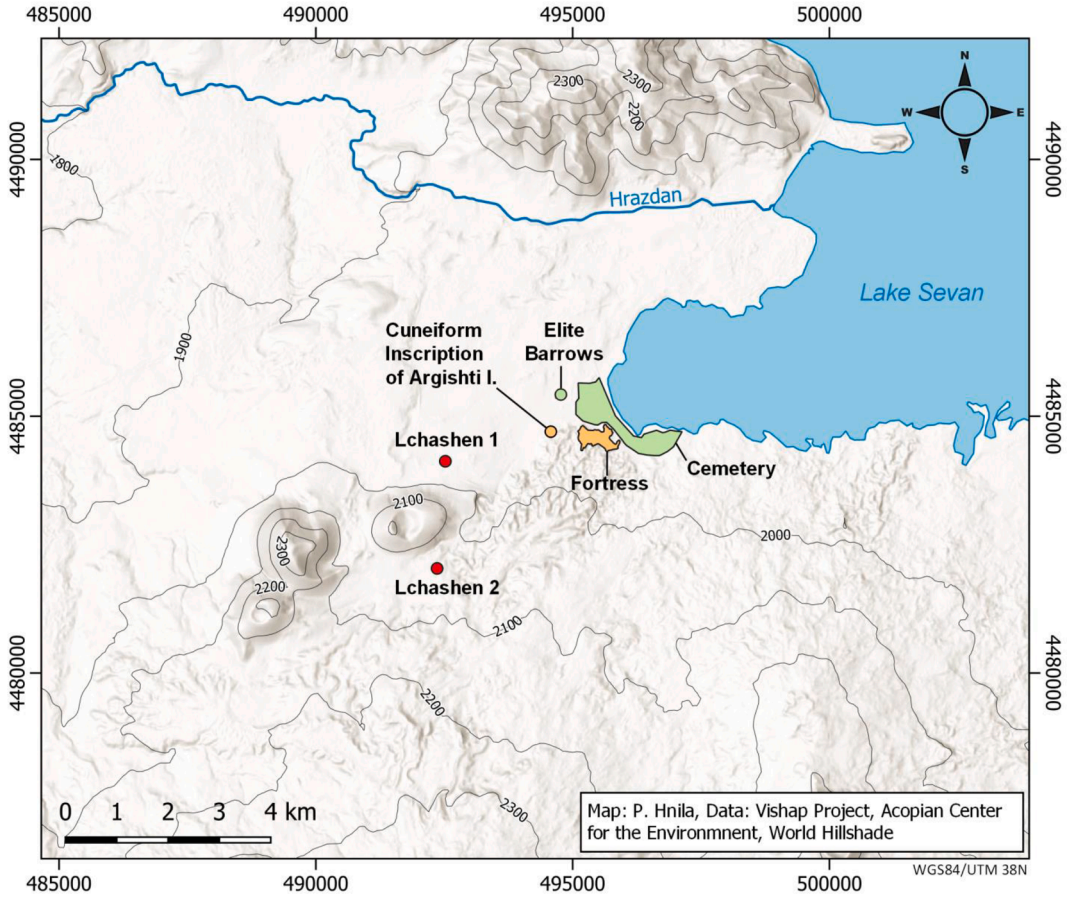

Fig. 2. Topographic map of Lchashen archaeological cluster with location of the dragon stones Lchashen 1 and 2 (P. Hnila).

of dark grey porous basalt; its size is 370x72x47 cm (Fig. 6). The waist widens upwards and the top is cut obliquely. The relief represents the hide of a bovid as if draped on the stela itself. The hide descends from the top of the stone to the back, ending in a tail with a multi-spiral bundle. The bovid's ears and the horns with arches descending on either side of the head are clearly distinguishable. A liquid flowing from the mouth of the bovid may represent water, blood, or a synecdoche of both (cf. Storaci and Gilibert, 2019).

3. Materials and methods

3.1. Osteological material

The human skeletal remains from the Lchashen barrow were inventoried at the Metsamor Historical-Archaeological Museum Reserve. The recent anthropological investigation of the remains as archived today revealed that they belong to two infants, hereinafter referred to as Dragon1 and Dragon2 (Fig. 5). These individuals were not accounted for in the original publication. Yet, a femur bone of a child is very likely identifiable on an archived field photograph of the excavation context. Another archived field photograph unequivocally proves that the tomb also contained an adult skull (published as Fig. 3 in Khanzadyan, 1995). However, neither this skull nor other adult bones are currently kept at the Metsamor Historical-Archaeological Museum Reserve. We could not find any trace of their current storage location. Supposedly, they were separated in 1980s and sent to Moscow to be studied by a Russian anthropologist Natalya Ermolova cooperating with Emma Khanzadyan.

The long bones of the upper and lower limbs (Table 1) of Dragon1 and Dragon2 were measured to estimate the biological ages of buried individuals, based on the method of V. Pashkova (1963). In addition, the degree of growth of deciduous teeth (hidden in the jaw or protruding from its broken parts) as well as the sizes of individual bones were measured according to the methods developed by B. Baker et al., (2010,157-165).

3.2. Radiocarbon dating

Originally, two samples underwent radiocarbon analyses at the Curt-Engelhorn Archaeometric Centre in Mannheim, Germany: one from the skull tentatively attributed to the Dragon1 individual (MAMS-32867) and one from a rib bone tentatively attributed to the Dragon2 individual (MAMS-34093). We consider attributions of Mannheim samples to respective individuals to be tentative, because after the sampling it became apparent that bones may have been found commingled and were separated into two skeletons only upon a later anthropological examination. According to the laboratory report from Mannheim, collagen was extracted from the bones and the >30kD fraction was separated with ultrafiltration. This fraction was freeze-dried and burned to CO_2 in an elemental analyzer. The resulting CO_2 was catalytically reduced to graphite. The radiocarbon values were measured in the accelerator mass spectrometer of the MICADAS type. Due to the chronological consistency issues, which emerged during the results evaluation, the archived collagen from both original samples was redated in the Mannheim laboratory under new laboratory numbers: MAMS-55173 for Dragon1, and MAMS-55174 for Dragon2.

To resolve issues with the tentative attribution to infant skeletons, two additional samples were taken from the left femurs of Dragon1 and Dragon2 – the same bones that were used for DNA analysis. They were analyzed under the numbers UGAMS-58597 (left femur of Dragon1) and UGAMS-58598 (left femur of Dragon2) in the Center for Applied Isotope Studies at the University of Georgia (CAIS) – with the additional goal of producing a cross-check for the samples dated in Mannheim. According

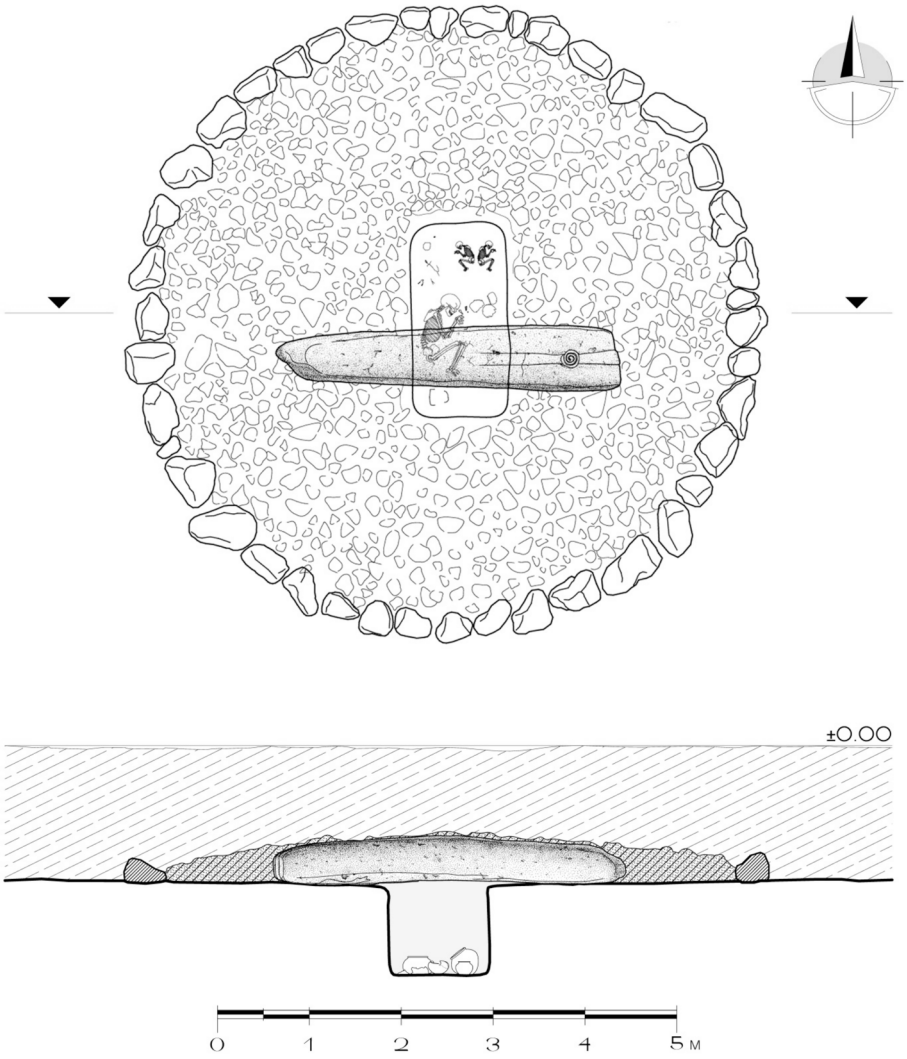

Fig. 3. Conjectural reconstruction of the dragon stone tomb. The indicated position of the skeletons and the pottery is based on evidence from field photographs and parallels from other coeval tombs at Lchashen (A. Hakhverdyan).

to the report by Alexander Cherkinsky, the bones analyzed in CAIS were cleaned by wire brush and washed, using ultrasonic bath. After cleaning, the dried bone was gently crushed into small fragments. The crushed bone was treated with 1 N HCl at 4° for 24 h. The residue was filtered, rinsed with deionized water and under slightly acid condition (pH = 3) heated at 80 °C for 6 h to dissolve collagen and leave humic substances in the precipitate. The collagen solution was then filtered to isolate pure collagen and dried out. The dried collagen was combusted at 575 °C in evacuated/sealed Pyrex ampoule in the present CuO. The resulting carbon dioxide was cryogenically purified from the other reaction products and catalytically converted to graphite using the method of Vogel et al. (1984). Graphite 14C/13C ratios were measured using the CAIS 0.5 MeV accelerator mass spectrometer. The sample ratios were compared to the ratio measured from the Oxalic Acid I (NBS SRM 4990).

All radiocarbon determinations received from Mannheim and CAIS were first calibrated individually in the OxCal software (Bronk Ramsey, 2009), version 4.4.4 from 2021, with atmospheric data from Reimer et al. (2020). Afterwards, given the archaeological premise of a single burial event (see sections "The Lchashen site and the dragon stone context" and "Discussion"), we combined the radiocarbon determinations into a chronological model within the OxCal software – using the contemporaneity of samples as a prior restraining factor. In comparison to the individually treated radiocarbon determinations, a combination of several determinations in chronological models usually leads to substantial improvements in terms of precision.

To factor in the differences between samples securely and tentatively attributed to specific individuals, in our model we achieved the combination by using two different methods. The first method – the *R_Combine* of the OxCal software – arithmetically averages individual determinations to produce a combined determination, which is subsequently calibrated; it is reserved for samples with the same radiocarbon reservoir, e.g., for remeasurements of the same sample or for samples from the same skeleton, or generally from a single source. The second method – *Combine* in the OxCal software – averages the probability distributions of individual determinations after they were already calibrated; it is used for multiple sources dating to the same event (for the use of both methods see Bronk Ramsey, 2005, ch. "Combination of Dates/Radiocarbon Dates"). Accordingly, in the first step we used *R_Combine* for MAMS-34093 and MAMS-55174, the only two determinations that remeasured the same sample twice and thus unequivocally represent the same individual. In the second step, we used the *Combine* method and nested the result from the first step together with the three determinations belonging to the same burial event but not necessarily to the same individual (MAMS-55173, UGAMS-58597, UGAMS-58598; see Table 2).

Fig. 4. Archaeological finds from the barrow with the dragon stone of Lchashen: 1–7 – dark-gray and painted pottery, 8 – bronze hair pin, 9 – carnelian bead, 10 – bone needle, 11 – fragment of obsidian (Courtisy of the Metsamor Historical-Archaeological Museum Reserve).

3.3. DNA extraction and sequencing

Materials and methods used. The ancient human remains samples were processed in dedicated clean laboratory facilities at the GLOBE Institute, University of Copenhagen, following established workflows designed to reduce the risk of contamination. Initially, we targeted the petrous bones for DNA extraction by isolating the densest part of the cochlea, which contains the highest endogenous DNA fraction (Gamba et al., 2014; Pinhasi et al., 2015). Each of the newborns had only one petrous bone remaining in the archaeological record: Dragon1 – right petrous, Dragon2 – left petrous. Since the individuals were buried together, in order to avoid the potentially wrong designation of the petrous bones to specific individuals, we also sampled the left femurs from each individual.

The drilled bone samples were divided into two different DNA lobind tubes per individual, each containing 100–200 mg of bone. DNA extractions were performed following a modified silica-in-solution protocol (Allentoft et al., 2015; Damgaard et al., 2015) and eluted in 64 μl of Qiagen's EB buffer. Two double-stranded libraries were generated from 32 μl of each extract following the BEST protocol, using adapters compatible with BGI sequencing according to Carøe et al., 2017; Mak et al., 2017. Quantitative real-time PCR (qPCR) was performed using SYBR green and Amplitaq Gold (Thermo Fisher) to estimate the required number of cycles for library index amplification. Each

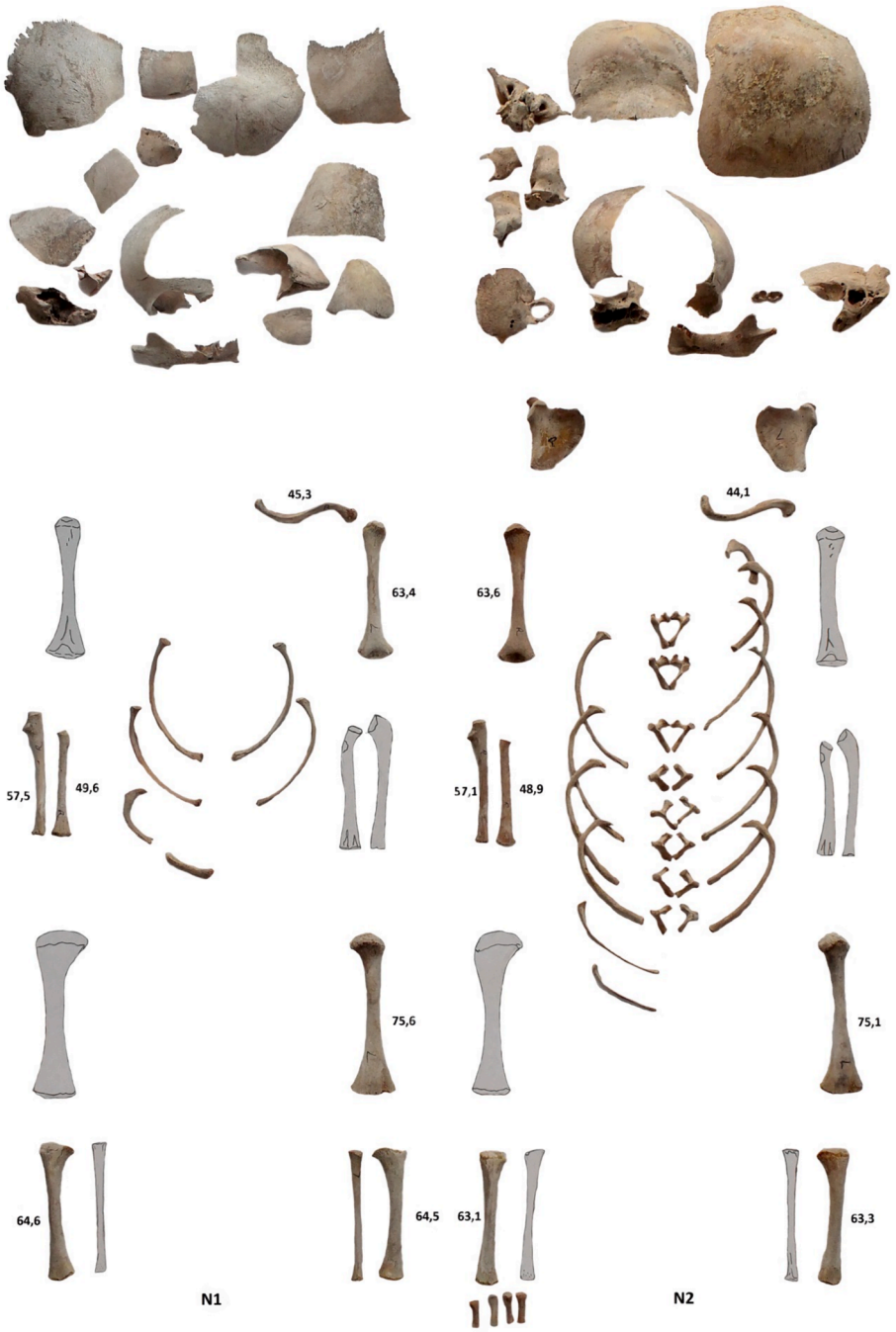

Fig. 5. Bones of the two newborn children from the barrow with dragon stone of Lchashen (H. Simonyan).

library was then double indexed and amplified using Amplitaq Gold (Thermo Fisher) and purified using SPRI beads as in (Rohland and Reich, 2012). The amplified libraries were quantified using the High-Sensitivity DNA Assay on an Agilent 2200 TapeStation (Agilent Technologies, Palo Alto, CA, USA). The amplified libraries were sequenced at BGISEQ-500 PE100.

Bioinformatics analysis and quality assessment. The PALEOMIX BAM workflow was used to process the raw fastq files (Schubert et al., 2014). In brief, BGI adaptors and stretches of Ns at both ends of the sequences were trimmed using AdapterRemoval v2.2 (Schubert et al., 2016), keeping only sequences with a minimum length of 30 bp. The trimmed sequences were mapped to the human reference genome build GRCh37 and the revised Cambridge reference sequence (rCRS, NCBI accession number NC_012920.1) using BWA v0.7.15 with "aln" algorithm (Li and Durbin, 2009) with the seed disabled allowing higher sensitivity (Schubert et al., 2012). We removed all the reads below mapping quality 30 and sorted the aligned sequences using Samtools v1.18 (Li et al., 2009). Duplicate sequences were filtered out by Picard MarkDuplicates (http://picard.sourceforge.net). The read length distribution and approximate Bayesian estimates of damage parameters were obtained using mapDamage v2.0 (Jónsson et al., 2013). We used contamMix for estimating the authentic fraction of DNA in ancient samples (Fu et al., 2013) and Picard CrosscheckFingerprints (https://picard.sourceforge.net) to verify the consistency of single libraries originating from the same individual.

Genetic sexing. We used the ratio of reads mapping to the Y chromosome (chrY) and X chromosome (chrX) to determine the sex of each sample as described in (Skoglund et al., 2013).

Fig. 6. Photo of the dragon stone of Lchashen 1 (erected at the entrance of the Metsamor Historical-Archaeological Museum Reserve) and its drawing on the right (A. Hakhverdyan).

Table 1
Maximum longitudinal dimensions (mm) of long bones of the skeletons of the Lchashen tomb with dragon stone, without epiphyses.

	Dragon1		Dragon2	
	Right	Left	Right	Left
Clavicle(Cl)	–	45.3	–	44.1
Humerus (H)	–	63.4	63.6	–
Radius (R)	49.6	–	48.9	–
Ulna (U)	57.5	–	57.1	–
Femur (F)	–	75.6	–	75.1
Tibia (T)	64.6	64.5	63.1	63.3

Mitochondrial genome analysis. To call the consensus mtDNA sequences, we aligned DNA reads from both individuals to the human mitochondrial reference genome: revised Cambridge Reference Genome (rCRS) with the same parameters as for the whole genome mapping. We applied base quality $\geq$ 20 and mapping quality $\geq$ 30 filters and only considered sites with at least "10×" coverage using bcftools mpileup | bcftools call pipeline. We then used haplogrep2 (Weissensteiner et al., 2016) for mtDNA haplogroup assignment. We finally inspected the sequences manually using Geneious Prime 2024 (https://www.geneious.com).

Genetic relatedness analysis. We assessed the genetic relatedness of the two individuals (four samples) by calculating estimating the 2dsfs through IBSrelate (Hanghøj et al. 2019; Waples et al. 2019). We ran IBSrelate using a minimum mapping quality of 30 and base quality of 20 as well as the sites with a minimum depth of 3 ("-setMinDepthInd 3″ in ANGSD). Additionally, we applied the KING software (Manichaikul et al., 2010) to the imputed dataset (explained below), assessing relatedness up to the second degree for all imputed genomes through the identification of segments Identical-by-State (IBS) and Identical-by-Descent (IBD) between pairs of individuals.

Imputation and IBD sharing. We imputed the genomes using GLIMPSE v1.1.185 (Rubinacci et al., 2021), employing the 1000G phase3 panel as a reference (Auton and Salcedo, 2015). To minimise batch effects, we imputed each genome individually. Subsequently, we filtered the imputed genomes based on established criteria (Sousa da Mota et al., 2023), which entailed excluding locations within repeat-rich regions and eliminating sites with QUAL < 30. Following this, we used IBDseq (Browning and Browning, 2013) on the imputed data to identify genomic segments shared identically-by-descent (IBD) within a reference panel of ancient genomes published in (Allentoft et al., 2024) and adhering to their criteria (LOD score $\geq$ 3, minimum length of 2 cM and removing regions of excess IBD).

Runs of Homozygosity (ROH). We estimated ROH using Plink (Purcell et al., 2007) and applying the parameters outlined by (Ceballos et al., 2018) (*–homozyg-snp 50 –-homozyg-kb 300 –-homozyg-density 50 –-homozyg-gap 100 –-homozyg-window-snp 50 –-homozyg-window-het 1 –-homozyg-window-threshold 0.05*).

Population genetics analyses. To assess the genetic relationship between the dragon stone tomb individuals and other ancient populations we combined the shotgun sequencing data of the two dragon stone genomes with previously published ancient and modern datasets based on the Affymetrix Human Origins SNP array (Allentoft et al., 2015; Broushaki et al., 2016; Cassidy et al., 2016; de Barros Damgaard et al., 2018; Fu et al., 2016; Haak et al., 2015; Haber et al., 2017; Harney et al., 2018; Hofmanová et al., 2016; Jones et al., 2015; Kılınç et al., 2016; Lamnidis et al., 2018; Lazaridis et al., 2014 and 2016; Martiniano et al., 2017; Mathieson et al., 2018, 2015; Mittnik et al., 2018; Narasimhan et al., 2019; Olalde et al., 2018; Sikora et al., 2019; Skoglund et al., 2017; Valdiosera et al., 2018; Wang et al., 2019). These included ancient individuals spanning from Late Paleolithic and Mesolithic until Iron Age from across Eurasia as well as an ancient individual from South Africa as an outgroup.

For obtaining the genotypes of the two ancient individuals from the dragon stone burial we used the "bcftools mpileup" command followed by a single read sampling of the major allele for each of the sites present in the comparative reference dataset, with mapping and base quality $\geq$ 30.

We used smartPCA (Patterson et al., 2006) implemented in EIGENSOFT v7.2 for conducting the principal components analysis (PCA) by projecting the ancient genomes (lsqproject: YES) onto the modern variation. The latter was inferred from a total of 769 present-day individuals from Europe, Caucasus and the Middle-East using n = 442,941 polymorphic sites. The ancient dataset was represented by the two samples from dragon stone burial along with 239 ancient individuals from 30 populations.

Table 2
Radiocarbon data from Lchashen "dragon stone" tomb.

Sample (laboratory number or OxCal command)	Object of analysis	Skeleton part	^{14}C age (years BP)	Year of analysis	δ^{13}C (‰) (Method)	C:N	C (%)	δ^{15}N (‰)	Collagen (%)	Unmodelled calibrated date, 95.4 % confidence range, years BC	Modelled calibrated date, 95.4 % confidence range, years BC
MAMS 32,867	Dragon1?	skull	3347 ± 22	2017	−9.5 (AMS)	2.6	41.6		2.6	1730–1721 (2.6 %) 1688–1539 (92.8 %)	outlier, not modelled
MAMS 34,093	Dragon2?	rib	3258 ± 23	2018	−21.8 (AMS)	2.9	37.9		7.6	1610–1576 (9.9 %) 1562–155 (1.7 %) 1547–1492 (71.1 %) 1482–1451 (12.7 %)	1600–1588 (5 %) 1544–1506 (90.5 %)
MAMS 55,173	MAMS-32867	skull	3268 ± 22	2022	−20.1 (AMS)	3.2	42.3			1612–1572 (17.9 %) 1566–1497 (74.0 %) 1474–1460 (3.6 %)	1600–1588 (5 %) 1544–1506 (90.5 %)
MAMS 55,174	MAMS-34093	rib	3291 ± 26	2022	−27.8 (AMS)	3.2	42.9			1614–1506 (95.4 %)	1600–1588 (5 %) 1544–1506 (90.5 %)
UGAMS 58,597	Dragon1	left femur	3280 ± 20	2022	−18.45 (IRMS)	3.20	66.48	12.12		1612–1572 (28.4 %) 1567–1502 (67.0 %)	1600–1588 (5 %) 1544–1506 (90.5 %)
UGAMS 58,598	Dragon2	left femur	3300 ± 20	2022	−18.44 (IRMS)	3.25	66.31	12.31		1616–1514 (95.4 %)	1600–1588 (5 %) 1544–1506 (90.5 %)
R_Combine (MAMS 34093 + MAMS 55174)	Dragon2?	rib	3273 ± 18	2023						1612–1572 (18.4 %) 1565–1500 (77.0 %)	1600–1588 (5 %) 1544–1506 (90.5 %)
Combine (all samples except MAMS 32867)	Dragon1 + 2	skull, rib, left femurs		2023						1600–1588 (5 %) 1544–1506 (90.5 %)	

Radiocarbon dates from the infants buried in the Lchashen dragon stone tomb, with the reported laboratory values and with the results calibrated in the OxCal software v.4.4.4 using the atmospheric data from Reimer et al., 2020. The code used for the chronological modelling is below the table.

Using a larger set of ancient pseudo-haploid individuals (n = 393) we conducted a maximum likelihood-based clustering analysis with ADMIXTURE (Alexander et al., 2009). After pruning the dataset for linkage disequilibrium using plink v1.9 with the settings (–indep-pairwise 50 10 0.1) the total number of SNPs was 167,968. We removed individuals from the analysis that had genotypes for less than 20 % of the SNPs, resulting in a total of 304 individuals. We used the program pong (Behr et al., 2016) to visualize the best run (out of 20 replicates) for each K and similar components between different Ks.

D-statistics estimates were computed with the ADMIXTOOLS (Patterson et al., 2012) and R package "admixr" (Petr et al., 2019) based on 189,406 transversions.

Metagenomic analysis. We screened reads not mapped to the human reference genome with the metagenomic profiler MALT (Herbig et al., 2016; Vågene et al., 2018) and the screening tool HOPS (Hübler et al., 2019) as implemented in the nf-core/eager pipeline (Fellows Yates et al., 2021), using standard parameters. Our reference panel included all complete bacterial and viral assemblies present in the NCBI as of July 2022. The resulting profiles were qualitatively assessed within HOPS for the number of aligning reads, the read edit distance against different taxa and the presence of aDNA damage patterns.

4. Results

4.1. Anthropological analyses

Anthropological analyses of the two individuals clearly indicate that both skeletons belonged to neonatal individuals in the age range of 0–2 months. The longitudinal dimensions of identical long bone from the two skeletons differ by 1.2 mm in the case of clavicle, 0.7 mm in the case of humerus, 0.4 mm in the case of radius, 0.5 mm in the case of femur while in the case of the tibia, as there are bones on the right and left sides, respectively by 1.5 and 1.2 mm (Table 1).

4.2. Chronological evaluation and radiocarbon dating

Based on comparative analysis of the corresponding tomb material (Fig. 4) – particularly the pottery vessels dating to the last phase of the Middle Bronze Age (Sevan-Artsakh and Karmir-Berd traditions) with some characteristics typical to the earliest stages of the Late Bronze Age – Emma Khanzadyan originally dated the tomb to the 16th-14th centuries BC (Khanzadyan, 2005). In one of her later manuscripts, she updated the dating of the tomb to a few centuries earlier: 17th-16th centuries BC (cf. Bobokhyan et al., 2017).

Khanzadyan's adjusted absolute chronological estimate fits remarkably well with the results of radiocarbon dating. Two left femur bones – the same ones confirmed by the genetic analysis as remains of second-degree relatives (see below) – were analyzed in the Center for Applied Isotope Studies at the University of Georgia (CAIS). The reported dates of 3280 ± 20 years BP for Dragon1 (UGAMS-58597) and 3300 ± 20 years BP for Dragon2 (UGAMS-58598) translate after their individual calibrations with 95.4 % probability to calendar years 1613–1503 BC for Dragon1 and 1616–1514 BC for Dragon2 (Fig. 7, Table 2).

Though the CAIS results of Dragon1 and Dragon2 radiocarbon samples by all standards cleanly overlap, their combined maximum possible span of 113 calendar years (1616–1503 BC) is rather broad and does not allow any decision about the contemporaneity of both individuals. It represents the most conservative estimate of the burial date in terms of absolute chronology. However, under the premise that both skeletons belong to a single burial event, the dating of the Lchashen tomb can be rendered more specific and more precise by incorporating radiocarbon determinations from Mannheim and by combining all available dates within a single chronological model.

Three Mannheim radiocarbon dates fit well with those obtained from CAIS: MAMS-55173 (3268 ± 22 years BP), MAMS-34093 (3258 ± 23 years BP), and MAMS-55174 (3291 ± 26 years BP), offering a welcome cross-check concerning the dating accuracy. The single exception is MAMS-32867 (3347 ± 22 years BP), which was confirmed as a laboratory outlier and thus excluded from further analysis (after the combination of first two Mannheim samples, MAMS-32867 and MAMS-34093,

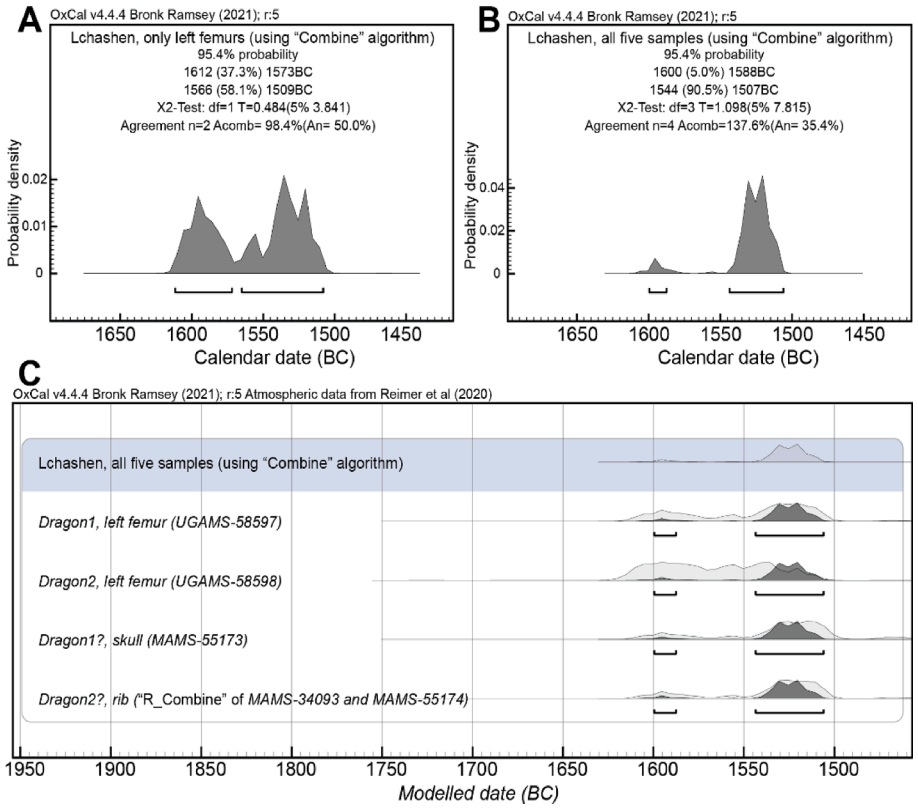

Fig. 7. Calibrated radiocarbon data from Lchashen "dragon stone" tomb. A) Plot of the modelled calibrated date combining exclusively UGAMS-58597 and UGAMS-58598 radiocarbon determinations from left femurs of Dragon1 and Dragon2 skeletons; B) Plot of the modelled calibrated date combining all five radiocarbon determinations from both skeletons as listed in C. In respect to A, it can be observed that the probabilities strongly shift towards the 2nd half of the 16th century BC. C) Plot of all radiocarbon determinations when combined under the premise of their contemporaneity. The uppermost light-grey distribution and the dark-grey distributions summarize the result of the entire combination, which is shown in detail in B. The light-grey color of four lower dates shows the original distribution of calendar age probabilities, before combining them. The horizontal bars show the position of the 95.4 % probability ranges.

failed to pass the chi-squared test in the OxCal model, the collagen from both samples was reanalyzed in the Mannheim lab; the new results revealed that MAMS-32867 does not fit with other three determinations from Mannheim and two determinations from CAIS).

As outlined in the methodology section, two determinations from CAIS and three determinations from Mannheim were combined into a single chronological model. The modelled result of the complete nested combination of all five radiocarbon determinations shows a distribution, which is at the 95.4 % confidence level remarkably uneven in respect to the individual calibrations: a statistical chance of only 5 % for a date between 1600 and 1588 BC, but astonishing 90.5 % for a date between 1544 and 1507 BC (Fig. 7, Table 2). Though none of these two calendar years ranges can be outright excluded, the combined distribution clearly leans towards the later range, with the probabilities reduced from 113 years (1616–1503 BC) to 12 + 37 years (1600–1588 and 1544–1507 BC) – a remarkable improvement in terms of precision. Given the second Millennium BC timescale and the uncertainties, all resulting dates should be rounded to decades. In conclusion, the infants buried in the Lchashen vishap tomb died in the 16th century BC, with a very high probability in its second half.

4.3. DNA data generation and authentication

Since neither the sex nor the biological relatedness between the newborn individuals could be determined using standard archaeological or anthropological methods, we applied ancient DNA (aDNA) techniques to provide new insights. We generated a total of ca. 3.1 billion DNA sequences using shotgun sequencing. The skeletal remains were remarkably well-preserved, exhibiting high levels of endogenous human DNA content ranging from 37 % to 52 %. This allowed for an average genomic coverage of 13.6x and 11.2x for Dragon1 and Dragon2 individuals, respectively. We observed typical aDNA read length distribution and deamination patterns for all samples, as well as low levels (<1%) of DNA contamination based on mtDNA analysis (Table S1 and S2). Interestingly, even though the average endogenous DNA fraction in petrous bones was higher than that of the femurs, this difference was not as large as expected from previous studies (Hansen et al., 2017). However, DNA damage profiles with lower deamination rates in the petrous bones may further support the higher DNA preservation rates in these parts of the skeletons.

4.4. Molecular sex, biological relatedness, parental relatedness and mitochondrial DNA analysis

Genetic sex determination based on X and Y chromosome reads revealed that both Dragon1 and Dragon2 were female.

Biological relatedness analysis revealed that the right and left petrous bones that allegedly originated from Dragon1 and Dragon2 samples, respectively, were genetically identical, indicating that either the two individuals were identical twins or that both petrous bones originated from the same individual. To address potential sample mix-ups due to proximity and disarticulated nature of the graves, we tested the genomes obtained from two left femurs from Dragon1 and Dragon2 to confirm they represent different individuals. Moreover, both petrous bones matched the femur sample from Dragon1, suggesting that all three bone fragments (right/left petrous bones and the left femur) originated from the same individual: Dragon1. Therefore, we combined the sequences from the petrous portions with the femur sample from

Dragon1 for downstream analyses. The genomes from Dragon1 and Dragon2 yielded an average coverage of 13.6x and 11.2x, respectively. The biological relatedness analysis conducted on the final, combined genomes indicated a second degree relationship, implying potential biological relations such as half-sisters, aunt-niece, double-cousins, or grandparent-grandchild (Table 3, Table S6).

Identifying segments identical-by-descent (IBD) between the two individuals helped us discard the double-cousin classification. Double cousins are anticipated to share both chromosomes IBD (IBD2) in 1/16 of their genomes (Ramstetter et al., 2018), yet no such segments were found in our data, as indicated in Fig. 8.

Distinguishing between half-sisters and aunt-niece relationships was impossible, given no additional relatives or individuals from the same population were available, therefore both half-sister or aunt-niece relationships are consistent with our data.

If they were half-sisters and shared the same mother, we would expect their maternally inherited mitochondrial genomes to be identical, as is seen here. However, the identical mitochondrial genomes also occur for paternally related siblings, if their mothers each had the same genome.

To further test if the two individuals shared a maternal or paternal link we examined their IBD shared segments. Due to sexual dimorphism in human meiotic recombination, females tend to transmit a larger number of smaller IBD segments compared to males (Bhérer et al., 2017). Maternal half-siblings, in particular, share approximately 1.4 times as many IBD segments on average as paternal half-siblings (Caballero et al., 2019). Based on this premise, we compared IBD sharing patterns in our individuals with previously published paternal half-brothers in (Schroeder et al., 2019). This analysis revealed that the two neonatal individuals buried at Lchashen shared 89 IBD chunks, ~1.4 times more than the half-brothers from Koszyce, which in average shared 66 IBD chunks (Table 4, Table S4). However, variations in the background population may influence the number of IBD chunks shared, making it uncertain whether the differences between the half-brothers from Koszyce and the half-sisters from Vishap are attributable to background population history or to differences in the common parent.

The absence of long Runs of Homozygosity (ROH) revealed that Dragon1 and Dragon2 did not originate from genetically related parents. Additionally, the absence of shorter ROH (>4cM) suggested they did not belong to a population with small effective population size, as shown in Table S5.

The mitochondrial sequences of both individuals were identical and belonged to the haplogroup U5a1a1 maternal lineage (Table S3). Among the ancient samples this mtDNA lineage is found in e.g. an Iron Age sample from Finland (DA234 (Sikora et al., 2019)); two Early Bronze Age Yamnaya individuals (SVP50 and SVP52 (Haak et al., 2015)); Bronze Age individual from Latvia (Kivutkalns153 (Mittnik et al., 2018)); Iron Age Germany (I12 (O'Sullivan et al., 2018)); Iron Age Finland (JK1968 and JK1970 (Lamnidis et al., 2018)); Afanasievo individual from Russia (RISE507) and Bell Beaker individual from Germany (RISE560) (Allentoft et al., 2015); Scythian individual from Moldova (SCY197 (Juras et al., 2017)).

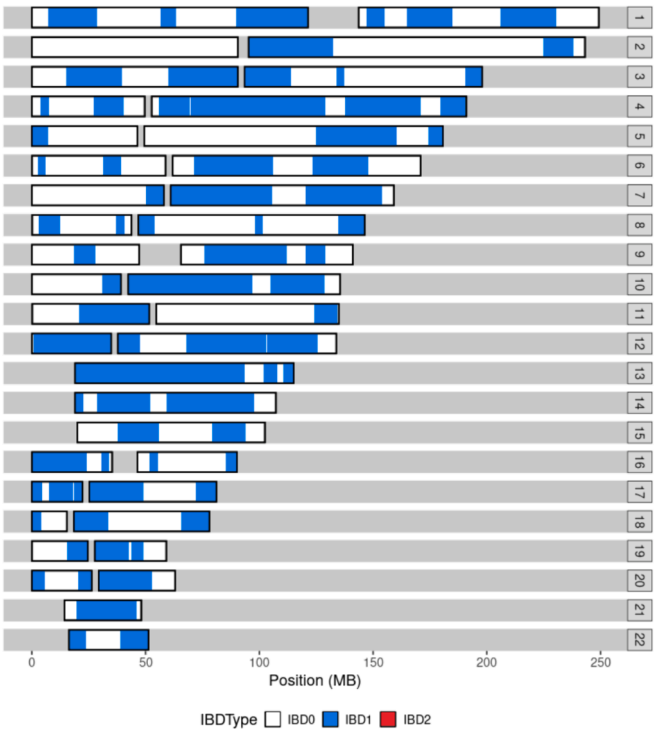

Fig. 8. IBD sharing patterns between Dargon1 and Dragon2 per chromosome.

Table 4
Genomic segments shared identically-by-descent (IBD).

Individual 1	Indindividual 2	nIBD	IBD length (cM)	Relatedness
RISE1163	RISE1168	63	2492.088339	Paternal half-brothers
RISE1163	RISE1169	68	2124.24765	Paternal half-brothers
RISE1173	RISE1168	61	2351.551708	Paternal half-brothers
RISE1173	RISE1169	72	2464.470657	Paternal half-brothers
Dragon1	**Dragon2**	**89**	**1324.783098**	**Half-sisters**

Number of IBD chunks (nIBD) and the total sum of IBD segments (IBD length (cM)) between pairs of individuals from Koszyce (Schroeder et al., 2019) and the Lchashen individuals (this study).

4.5. *Genetic affinities*

We analysed the genetic relationship between the two individuals of the burial with dragon stone stela at the site Lchashen and other ancient populations from the region to assess whether these individuals buried in the tomb were possibly of a different genetic background. The comparative dataset included Chalcolithic, Bronze Age and Iron Age individuals from Armenia as well as various populations from Eurasia ranging from Mesolithic until Iron Age for a broader context.

Table 3
Pairwise genetic relatedness.

Sample	Sample	nSites	R0	R1	KING	Relatedness
Dragon1_Femur	Dragon1_Petrous	262,766	0	2.678	0.421	Identical
Dragon1_Femur	Dragon2_Femur	724,563	0.166	0.403	0.155	Second degree
Dragon1_Femur	Dragon2_Petrous	424,817	0	2.96	0.428	Identical
Dragon1_Petrous	Dragon2_Femur	265,602	0.191	0.318	0.125	Second degree
Dragon1_Petrous	Dragon2_Petrous	186,931	0	2.724	0.422	Identical
Dragon2_Femur	Dragon2_Petrous	427,281	0.189	0.333	0.129	Second degree

We used the known variable transversion sites from the 1000 Genomes project to estimate the R0, R1 and KING-robust kinship statistics implemented in IBSrelate. nSites shows the number of sites with three-fold and above coverage which were used for the IBSRelate analysis.

The results clearly show that based on the PCA and ADMIXTURE analysis the individuals from the Lchashen burial form a group together with other Bronze Age individuals from Armenia (Fig. 9).

4.6. Pathogen screening

We were unable to identify any endoparasites or viral/bacterial infectious agents that could account for the death of the individuals, as the non-human sequences mainly originate from the environment.

5. Discussion

5.1. Anthropological evidence

Anthropological evidence proves that the two skeletons belonged to individuals of identical age sharing a nearly identical growth pattern. Small differences in the maximum longitudinal dimensions of identical long bones of the two skeletons could be the result of differentiated intrauterine growth and unequal distribution of food resources. Such an observation was documented at the site Olerdola in Barcelona, 4th-2nd centuries BC. The skeletons of the two-week-old Olerdola children were studied by the orthodontic method. They show a discrepancy between identical bone sizes of up to 5 mm, considering it to be the result of an asymmetry of intrauterine growth of normal couples (Crespo et al., 2011; for modern observations on the birth weight and fertilization temporal distance of twins cf. Mogollón et al., 2020). Differences in dimension between other bones of the two skeletons do not reach 2 mm, which again stands well within the range of possible intrauterine growth differences.

An alternative explanation for the differences in bone dimensions

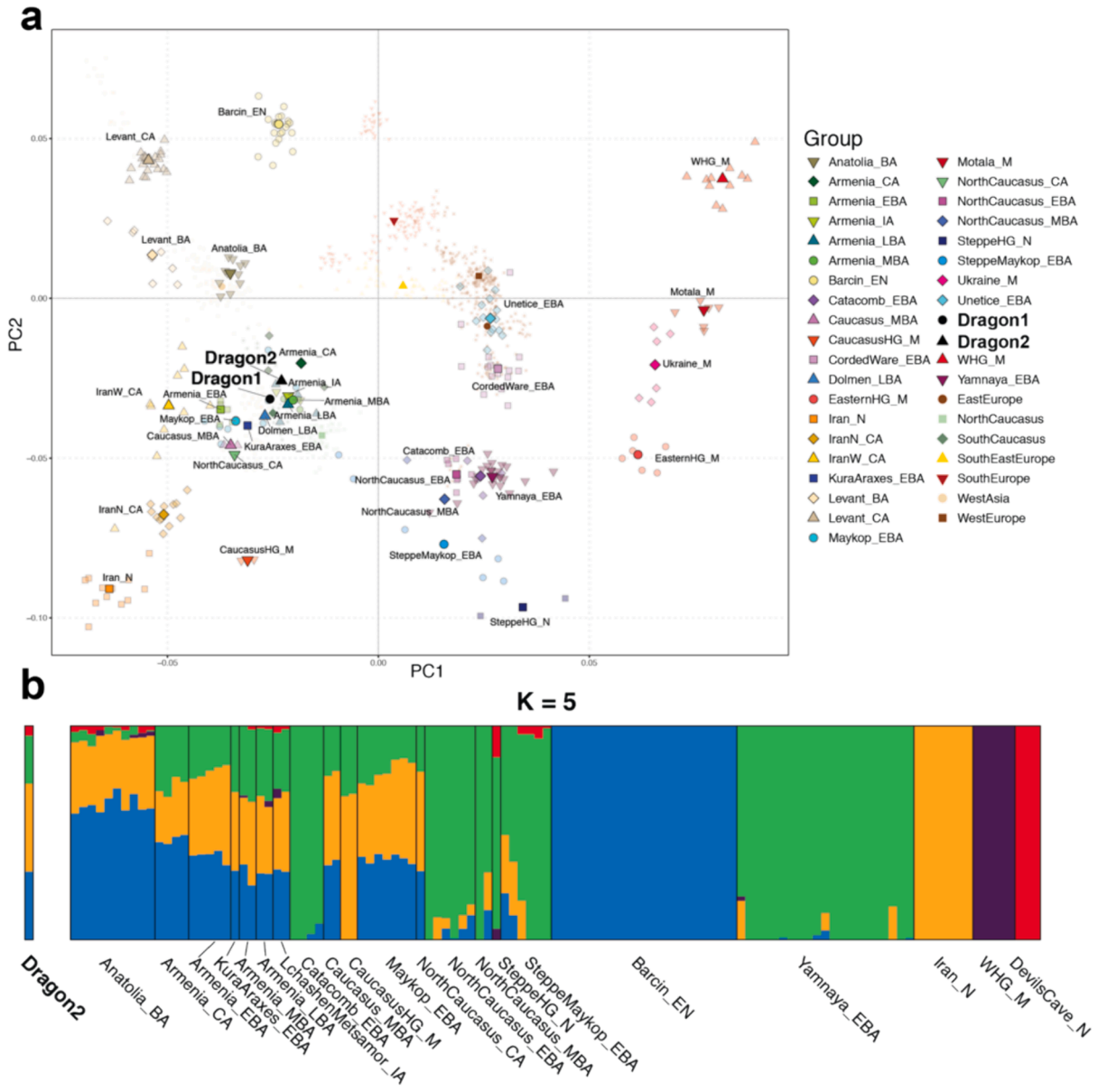

Fig. 9. PCA and admixture analyses. A) PCA analysis of the two dragon stone individuals (Dragon1 and Dragon2) and relevant comparative ancient populations from Eurasia ranging from Mesolithic till Iron Age. The ancient genomes were projected onto the modern variation based on the HO panel of populations from Europe, Near East and Caucasus. B) Unsupervised clustering analysis using ADMIXTURE, (K=5) to estimate ancestry proportions of Dragon2 individual. Since the two dragon stone individuals were related we only used the sample with the highest depth of coverage i.e., Dragon2. A total of 300 individuals with 190,111 SNPs markers were used for the analysis. Similarly, model-based clustering analysis using Admixture revealed that the genetic ancestry of Dragon1 and Dragon2 individuals were similar to that of Bronze Age Armenia and Caucasus (Maykop and Kura-Araxes cultures).

may be variation in birth weight, as has been reported for twins originating from superfecundation, and which were interpreted as a consequence of the time passed between the two fertilizations (Jonczyk, 2015, 35).

5.2. Dating the time of death by radiocarbon

The simultaneous death of the two individuals can be neither confirmed, nor excluded on the basis of the radiocarbon dating alone. It should be stressed that confirming simultaneous deaths from dated bones is beyond the reach of the radiocarbon method, since the uncertainties caused by the calibration curve are currently larger than a single human generation. Even in the best possible scenario, in the case of a single bone from the middle of the 16th century BC being repeatedly dated by radiocarbon in the same laboratory with an unrealistic certainty of one radiocarbon year, the resulting range after calibration in calendar years would cover half a century or more (tested with ten simulations in the OxCal software with *R_Simul*ate command using the calendar date of 1550 BC with uncertainty of 1 year).

5.3. Genetic evidence and archaeological interpretation

The genomic analysis of the two newborn females from the "dragon stone" tomb indicates that they were second-degree related, sharing 25 % of their DNA. Biologically speaking, this may result from the two individuals being (a) half-sisters, (b) aunt (likely maternal) and niece, (c) double-cousins or (d) grandmother (likely maternal) and granddaughter. The option (c) double-cousins was rejected based on the IBD results. However, without additional related individuals or references from the same population, it's challenging to differentiate between these remaining categories solely based on genetic data.

From the archaeological perspective, most of these options are expected to occur in multi-generational tombs, repeatedly reopened for the inhumation of members of extended families or small communities. However, multi-generational tombs are not attested among the over 400 tombs excavated at Late Bronze Age Lchashen, nor are they in any other contemporary necropolis in Armenia. Additionally, the dragon stone tomb lacks the defining characteristics of multi-generational burials, such as architectural features allowing the easy recursive reopening of the burial chamber (a dromos, a door, a built stone cist etc.), significant quantities of older bones selected and curated in specific collection areas and artefacts dating to a longer period of time. On the contrary, the inventory, the all-encompassing pattern of bone dispersal, and the radiocarbon dating of the Lchashen dragon stone barrow are consistent with a single-event burial robbed in antiquity, which is the norm for the Middle and Late Bronze Age.

If indeed the infants' burial occurred in one event, the scenarios listed above are exceptionally rare or, in one case, impossible. Considered case by case:

(a) If the individuals were half-sisters sharing the same mother as suggested by the mitochondrial genome and IBD analysis combined, it would imply heteropaternal superfecundation.
(b) If the individuals were aunt and niece, the scenario implies one parent and her/his offspring each having a daughter and losing her at the same time.
(c) We discard the possibility of the simultaneous birth of a grandparent and a grandchild.

The event envisaged by the burial is in any case exceptional, both from the point of view of genetics and from the archaeological viewpoint. In Late Bronze Age Armenia in general and at Lchashen in particular, burials of children are rare and the burial of two newborns combined with a monumental stela is unique.

The loss of the adult skeletal remains originally retrieved from the tomb deprives us of an important genetic source to further narrow down the possible scenarios. However, two observations may suggest that the adult skeleton was female. First, the excavator noted that the skeleton was found lying on its left side (Khanzadyan, 2005, 89). According to anthropological analyses, the position of bodies buried at the Late Bronze Age Lchashen cemetery depends on their sex, with male bodies laid down on their right side and female bodies laid down on their left side (Vardanyan, 2019, 68). Second, the bronze hair-ring found under the adult skull is of a type that needs to be interwoven into long hair or braids. In Late Bronze Age Eurasia, it was typically (though not exclusively) worn by females, seen in the Balkans (Zaharia, 1959, 105) and in Germany (Schwarz, 2014, 724). No similar evaluations exist yet from the Caucasus.

We can thus reasonably expect that the Dragon1 and Dragon2 individuals were buried with a female. If the genomic evidence were lacking, archaeologists would almost certainly interpret this peculiar context as the burial of a mother and her twin offspring, likely victims of one of the most widespread causes of death in ancient times: childbirth death. However, the presence of the dragon stone and the location of the graves outside the main cemetery distinguish this burial from other burials of the time. The genomic evidence, which reveals the biological sex and an unexpected degree of relatedness, adds a further level of uniqueness to the context and may offer a possible key to better understanding it.

5.4. The evidence from socio-anthropological perspective

In the South Caucasus, stelae are sometimes used to mark graves. However, out of 454 Bronze Age graves excavated at Lchashen (Petrosyan, 2018, 7), not one was marked by any kind of stelae. Only this grave was marked with a dragon stone. We hypothesize that the stela was put on this tomb because the twin children were considered extraordinary (for the topic cf. Abrahamian, 1983, 131-186), a phenomenon which could have enhanced the uniqueness of the event.

In this perspective the question, how did the newborns die, becomes more intriguing. The possibilities are two: they died naturally or were killed/sacrificed. The burial may be the result of a difficult birth, at the end of which the twins died. However, both the widespread spirituality among ancient societies and an unparalleled symbolic connotation of the burial with a dragon stone, raise the possibility of a sacred killing, although no direct traces of violence were detected on the fragile infant remains. The killing of twins at birth is a wide-spread cultural phenomenon (cf. Abrahamian, 1977, 181). In some ancient traditions are known also graves of twins to be located on lake shores (cf. Ivanov, 1991, 176; Zakaryan, 2014, 76). This context raises the possibility that the Lchashen newborns were perhaps sacrificed in a ritual connected to the zoomorphic statue.

6. Conclusions

In the 16th century BC, a three and half meter high stela of basalt with an image of sacrificed bovid was put on a barrow in Lchashen, in a plateau overlooking Lake Sevan, in present-day Armenia. The pit of the burial contained archaeological material as well as human bones of an adult (supposedly female) and two newborns at the age of 0 to 2 months. Nearly identical bone sizes of those children implied the possibility of a twin burial. This primary assumption was tested by ancient DNA analyses, which showed that the two female individuals were second-degree related and display genetic ancestry profiles similar to that of other Bronze Age individuals from the South Caucasus. Archaeologically, second-degree related infants (possibly half-siblings) have never been

attested[1]: in this context, the case of Lchashen seems to be of special interest. We argue that the reason for placing such an impressive monument on the burial of two newborns is that they were considered extraordinary.

CRediT authorship contribution statement

Arsen Bobokhyan: Conceptualization, Data curation, Writing – original draft, Writing – review & editing, Investigation, Project administration, Funding acquisition, Supervision. **Miren Iraeta-Orbegozo:** Data curation, Software, Writing – original draft, Writing – review & editing, Investigation, Methodology, Formal analysis. **Hugh McColl:** Data curation, Software, Writing – review & editing. **Ruzan Mkrtchyan:** Investigation, Anthropological data curation. **Hasmik Simonyan:** Anthropological data curation, Writing – original draft. **Jazmín Ramos-Madrigal:** Supervision, Writing – review & editing. **Aída Andrades-Valtueña:** Supervision, Writing – review & editing. **Pavol Hnila:** Writing – Original draft, Investigation, Funding acquisition, Writing – Review & Editing. **Alessandra Gilibert:** Writing – original draft, Investigation, Writing – review & editing. **Ashot Margaryan:** Conceptualization, Writing – original draft, Investigation, Writing – review & editing.

Declaration of competing interest

The authors declare that they have no known competing financial interests or personal relationships that could have appeared to influence the work reported in this paper.

Data availability

The aligned sequence data (BAM format; after MAPQ 30, length filter 30 bp and removal of duplicates) reported in this paper can be accessed through the European Nucleotide Archive under the project name: PRJEB74217.

Acknowledgements

We express our gratitude to the Metsamor Historical-Archaeological Museum Reserve, Armenia (director Artavazd Zakyan) for permission to work with materials from Lchashen as well as to the Institute of Archaeology and Ethnography (director Pavel Avetisyan) and Service for the Protection of the Historical Environment and Cultural Museum-Reservations, Armenia (Scientific director Ashot Piliposyan) for supporting our undertaking. For essential hints we thank Sargis Hayotsyan, Chairman of the Higher Education and Science Committee, RA MESCS, as well as cultural anthropologists Levon Abrahamian, Armen Petrosyan and Tork Dalalyan. Ray Kidd and Erik Marsh offered helpful comments on using OxCal methods. The archaeological part of the work has been realized in the frames of the Higher Education and Science Committee, RA MESC grant no. 21AG-6A080; the UGAMS radiocarbon dates were funded by the Deutsche Forschungsgemeinschaft (DFG, German Research Foundation), project number 462731233; the open access was possible by funding of Ca' Foscari University of Venice. A special thanks to Thomas P. Gilbert for his support with the project.

Appendix A. Supplementary data

Supplementary data to this article can be found online at https://doi.org/10.1016/j.jasrep.2024.104601.

[1] For other newborn twin burials cf. Krems-Wachtberg (ca. 27.000 BP, Teschler-Nicola et al., 2020), Irkutsk (ca. 8000 BP, Mazza, 2015), La Brania (ca. 8000 BP, Zimmer, 2019), Ochtendung (first half of the 1st millennium BC, Flohr, 2012), Olerdola (4th-2nd centuries BC, Crespo et al., 2011).

References

Abrahamian, L.A., 1977. Towards the Idea of doppelganger, according to some ethnographical and folkloristic evidence. Historical-Philological Journal 2, 177–190 in Russian.
Abrahamian, L.A., 1983. Primitive Festival and Mythology. Academy of Sciences Press, Yerevan (in Russian).
Alexander, D.H., Novembre, J., Lange, K., 2009. Fast model-based estimation of ancestry in unrelated individuals. Genome Res. 19 (9), 1655–1664.
Allentoft, M.E., Sikora, M., Sjögren, K.-G., Rasmussen, S., Rasmussen, M., Stenderup, J., Willerslev, E., 2015. Population genomics of Bronze Age Eurasia. Nature 522 (7555), 167–172.
Allentoft, M.E., Sikora, M., Refoyo-Martínez, A., et al., 2024. Population genomics of post-glacial western Eurasia. Nature 625, 301–311. https://doi.org/10.1038/s41586-023-06865-0.
Auton, A., Salcedo, T., 2015. The 1000 genomes project. In: Assessing Rare Variation in Complex Traits: Design and Analysis of Genetic Studies. Springer, New York, pp. 71–85. https://doi.org/10.1007/978-1-4939-2824-8_6.
Baker, B.J., Dupras, T.L., Tocheri, M.W., 2010. The Osteology of Infants and Children, Second Edition. University Press, Texas.
Behr, A.A., Liu, K.Z., Liu-Fang, G., Nakka, P., Ramachandran, S., 2016. Pong: fast analysis and visualization of latent clusters in population genetic data. Bioinformatics 32 (18), 2817–2823.
Bhérer C., Campbell C.L., Auton A., 2017. Refined genetic maps reveal sexual dimorphism in human meiotic recombination at multiple scales. Nat Commun. Apr 25; 8:14994. doi: 10.1038/ncomms14994.
Bobokhyan, A., Gilibert, A., Hnila, P., 2015. Archaeology of vishap stones. In: Petrosyan, A., Bobokhyan, A. (Eds.), Vishap Stones. Academy of Sciences Press, Yerevan, pp. 269–396 in Armenian.
Bobokhyan, A., Piliposyan, A., Mkrtchyan, R., Simonyan, H., Zakyan, A., 2017. Emma Khanzadyan and the investigation of vishap stones. In: Piliposyan, A. (Ed.), Metsamorian Readings 1. Service for the Protection of Historical Environment and Cultural Museum Reservations SNCO, Yerevan, pp. 93–122 in Armenian.
Bobokhyan, A., Gilibert, A., Hnila, P., 2018. Karmir Sar: new evidence on dragon stones and ritual landscapes on Mount Aragats, Armenia. In: Batmaz, A., Bedianashvili, G., Michalewicz, A., Robinson, A. (Eds.), Context and Connection: Essays on the Archaeology of the Ancient near East in Honour of Antonio Sagona, Orientalia Lovaniensia Analecta 268. Peeters, Leuven - Paris - Bristol, pp. 255–270.
Bronk Ramsey, Ch., 2009. Bayesian analysis of radiocarbon dates. Radiocarbon 51, 337–360.
Bronk Ramsey, Ch., 2005. OxCal program v3.10 manual. https://c14.arch.ox.ac.uk/oxcal3/oxcal.htm.
Broushaki, F., Thomas, M.G., Link, V., López, S., van Dorp, L., Kirsanow, K., Burger, J., 2016. Early Neolithic genomes from the eastern Fertile Crescent. Science 353 (6298), 499–503.
Browning B.L., Browning S.R., 2013. Improving the accuracy and efficiency of identity-by-descent detection in population data. Genetics. Jun;194(2): 459–471. doi: 10.1534/genetics.113.150029.
Caballero, M., Seidman, D.N., Qiao, Y., Sannerud, J., Dyer, T.D., Lehman, D.M., et al., 2019. Crossover interference and sex-specific genetic maps shape identical by descent sharing in close relatives. PLoS Genet 15 (12), e1007979.
Cassidy, L.M., Martiniano, R., Murphy, E.M., Teasdale, M.D., Mallory, J., Hartwell, B., Bradley, D.G., 2016. Neolithic and Bronze Age migration to Ireland and establishment of the insular Atlantic genome. Proceedings of the National Academy of Sciences of the United States of America 113(2), 368–373.
Ceballos, F.C., Joshi, P.K., Clark, D.W., Ramsay, M., Wilson, J.F., 2018. Runs of homozygosity: windows into population history and trait architecture. Nat. Rev. Genet. 19, 220–234.
Crespo, L., Subira, M., Ruiz, J., 2011. Twins in prehistory: the case from Olèrdola (Barcelona, Spain, c. IV–II BC). Int. J. Osteoarchaeol. 21 (6), 751–756.
Damgaard, P.B., Margaryan, A., Schroeder, H., Orlando, L., Willerslev, E., Allentoft, M.E., 2015. Improving access to endogenous DNA in ancient bones and teeth. Sci. Rep. 5, 11184.
de Barros Damgaard, P., Martiniano, R., Kamm, J., Moreno-Mayar, J.V., Kroonen, G., Peyrot, M., Willerslev, E., 2018. The first horse herders and the impact of early Bronze Age steppe expansions into Asia. Science 360 (eaar7711). https://doi.org/10.1126/science.aar7711.
Fellows Yates J.A., Lamnidis T.C., Borry M., Andrades Valtueña A., Fagernäs Z., Clayton S., Garcia M.U., Neukamm J., Peltzer A., 2021. Reproducible, portable, and efficient ancient genome reconstruction with nf-core/eager. PeerJ. Mar 16;9:e10947. doi: 10.7717/peerj.10947.
Flohr, S., 2012. Twin burials in prehistory: a possible case from the Iron Age of Germany. International Journal of Osteoarchaeology. DO I, 2012. https://doi.org/10.1002/oa.2236, Wiley Online Library, First published: 01 Match.
Fu, Q., Mittnik, A., Johnson, P.L.F., Bos, K., Lari, M., Bollongino, R., Krause, J., 2013. A revised timescale for human evolution based on ancient mitochondrial genomes. Curr. Biol. 23 (7), 553–559.
Fu, Q., Posth, C., Hajdinjak, M., Petr, M., Mallick, S., Fernandes, D., Reich, D., 2016. The genetic history of Ice Age Europe. Nature 534 (7606), 200–205.
Gamba, C., Jones, E.R., Teasdale, M.D., McLaughlin, R.L., Gonzalez-Fortes, G., Mattiangeli, V., Pinhasi, R., 2014. Genome flux and stasis in a five millennium transect of European prehistory. Nat. Commun. 5, 5257.
Gilibert, A., Bobokhyan, A., Hnila, P., 2012. Dragon stones in context: the discovery of high-altitude burial grounds with sculpted stelae in the Armenian mountains. Mitteilungen der Deutschen Orient-Gesellschaft 144, 93–132.

Haak, W., Lazaridis, I., Patterson, N., Rohland, N., Mallick, S., Llamas, B., Reich, D., 2015. Massive migration from the steppe was a source for Indo-European languages in Europe. Nature 522 (7555), 207–211.
Haber, M., Doumet-Serhal, C., Scheib, C., Xue, Y., Danecek, P., Mezzavilla, M., Tyler-Smith, C., 2017. Continuity and admixture in the last five millennia of Levantine history from Ancient Canaanite and present-day Lebanese genome sequences. Am. J. Hum. Genet. 101 (2), 274–282.
Hanghøj, K., Moltke, I., Andersen, P.A., Manica, A., Korneliussen, T.S., 2019. Fast and accurate relatedness estimation from high-throughput sequencing data in the presence of inbreeding. GigaScience 8 (5). https://doi.org/10.1093/gigascience/giz034.
Hansen, H.B., Damgaard, P.B., Margaryan, A., Stenderup, J., Lynnerup, N., Willerslev, E., Allentoft, M.E., 2017. Comparing Ancient DNA Preservation in Petroud Bone and Tooth Cementum. PLoS One. https://doi.org/10.1371/journal.pone.0170940.
Harney, É., May, H., Shalem, D., Rohland, N., Mallick, S., Lazaridis, I., Reich, D., 2018. Ancient DNA from Chalcolithic Israel reveals the role of population mixture in cultural transformation. Nat. Commun. 9 (1), 3336.
Herbig, A., Maixner, F., Bos, K.I., Zink, A., Krause, J., Huson, D.H., 2016. MALT: Fast alignment and analysis of metagenomic DNA sequence data applied to the Tyrolean Iceman. bioRxiv:050559. DOI: 10.1101/050559.
Hnila, P., Gilibert, A., Bobokhyan, A., 2019. Prehistoric sacred landscapes in the high mountains: the case of the vishap stelae between Taurus and Kaukasus. In: Engels, B., Huy, S., Steitler, Ch. (Hrsg.), Natur und Kult in Anatolien, BYZAS 24: Veröffentlichungen des Deutschen Archäologischen Instituts Istanbul, Istanbul, pp. 283-302.
Hofmanová, Z., Kreutzer, S., Hellenthal, G., Sell, C., Diekmann, Y., Díez-Del-Molino, D., Burger, J., 2016. Early farmers from across Europe directly descended from Neolithic Aegeans. PNAS 113 (25), 6886–6891.
Hübler, R., Key, F.M., Warinner, C., et al., 2019. HOPS: automated detection and authentication of pathogen DNA in archaeological remains. Genome Biol 20, 280. https://doi.org/10.1186/s13059-019-1903-0.
Ivanov, V.V., 1991. Twin myths. In: Tokarev, S.A. (Ed.), Myths of the Peoples of the World, vol. 1. Soviet Encyclopaedia, Moscow, pp. 174–177 in Russian.
Jonczyk, P., 2015. Superfecundadtion – from ancient to modern times. Ginekologia i Położnictwo Medical Project 4 (38), 32–39.
Jones, E.R., Gonzalez-Fortes, G., Connell, S., Siska, V., Eriksson, A., Martiniano, R., Bradley, D.G., 2015. Upper Palaeolithic genomes reveal deep roots of modern Eurasians. Nat. Commun. 6, 8912.
Jónsson, H., Ginolhac, A., Schubert, M., Johnson, P.L.F., Orlando, L., 2013. mapDamage2.0: fast approximate Bayesian estimates of ancient DNA damage parameters. Bioinformatics 29, 1682–1684. https://doi.org/10.1093/bioinformatics/btt193.
Juras, A., Krzewińska, M., Nikitin, A.G., Ehler, E., Chyleński, M., Łukasik, S., Götherström, A., 2017. Diverse origin of mitochondrial lineages in Iron Age Black Sea Scythians. Sci. Rep. 7, 43950.
Khanzadyan, E., 2005. The vishap of Lchashen. In: Kalantaryan, A., Badalyan, R., Avetisyan, P. (Eds.), Culture of Ancient Armenia XIII. Academy of Sciences Press, Yerevan, pp. 86–91 in Armenian.
Kılınç, G.M., Omrak, A., Özer, F., Günther, T., Büyükkarakaya, A.M., Bıçakçı, E., Götherström, A., 2016. The demographic development of the first farmers in Anatolia. Curr. Biol. 26 (19), 2659–2666.
Lamnidis, T.C., Majander, K., Jeong, C., Salmela, E., Wessman, A., Moiseyev, V., Schiffels, S., 2018. Ancient Fennoscandian genomes reveal origin and spread of Siberian ancestry in Europe. Nat. Commun. 9 (1), 5018.
Lazaridis, I., Patterson, N., Mittnik, A., Renaud, G., Mallick, S., Kirsanow, K., Krause, J., 2014. Ancient human genomes suggest three ancestral populations for present-day Europeans. Nature 513 (7518), 409–413.
Lazaridis, I., Nadel, D., Rollefson, G., Merrett, D.C., Rohland, N., Mallick, S., Reich, D., 2016. Genomic insights into the origin of farming in the ancient Near East. Nature 536 (7617), 419–424.
Li, H., Durbin, R., 2009. Fast and accurate short read alignment with Burrows-Wheeler transform. Bioinformatics 25 (14), 1754–1760.
Li, H., Handsaker, B., Wysoker, A., Fennell, T., Ruan, J., Homer, N., 2009. 1000 genome project data processing subgroup. The sequence alignment/map format and SAMtools. Bioinformatics 25 (16), 2078–2079.
Mak, S.S.T., Gopalakrishnan, S., Carøe, C., Geng, C., Liu, S., Sinding, M.H.S., Kuderna, L. F.K., Zhang, W., Fu, S., Vieira, F.G., Germonpré, M., Bocherens, H., Fedorov, S., Petersen, B., Sicheritz-Pontén, T., Marques-Bonet, T., Zhang, G., Jiang, H., Gilbert, M.T.P., 2017. Comparative performance of the BGISEQ-500 vs Illumina HiSeq2500 sequencing platforms for palaeogenomic sequencing. GigaScience 6, 1–13.
Manichaikul, A., Mychaleckyj, J.C., Rich, S.S., Daly, K., Sale, M., Chen, W.M., 2010. Robust relationship inference in genome-wide association studies. Bioinformatics 26, 2867–2873.
Martiniano, R., Cassidy, L.M., Ó'Maoldúin, R., McLaughlin, R., Silva, N.M., Manco, L., Bradley, D.G., 2017. The population genomics of archaeological transition in west Iberia: Investigation of ancient substructure using imputation and haplotype-based methods. PLoS Genet. 13 (7), e1006852.
Mathieson, I., Lazaridis, I., Rohland, N., Mallick, S., Patterson, N., Roodenberg, S.A., Reich, D., 2015. Genome-wide patterns of selection in 230 ancient Eurasians. Nature 528 (7583), 499–503.
Mathieson, I., Alpaslan-Roodenberg, S., Posth, C., Szécsényi-Nagy, A., Rohland, N., Mallick, S., Reich, D., 2018. The genomic history of southeastern Europe. Nature 555 (7695), 197–203.
Mazza, E., 2015. Ancient grave in Siberia yields earliest example of twins. Science 02 (05), 08:41 am.
Mittnik, A., Wang, C.-C., Pfrengle, S., Daubaras, M., Zariņa, G., Hallgren, F., Krause, J., 2018. The genetic prehistory of the Baltic Sea region. Nat. Commun. 9 (1), 442.
Mogollón, F., Casas-Vargas, A., Rodríguez, F., Usaquén, W., 2020. Twins from different fathers: A heteropaternal superfecundation case report in Colombia. Biomedica 40 (4), 604–608.
Narasimhan, V.M., Patterson, N., Moorjani, P., Rohland, N., Bernardos, R., Mallick, S., Reich, D., 2019. The formation of human populations in South and Central Asia. Science 365 (6457). https://doi.org/10.1126/science.aat7487.
Olalde, I., Brace, S., Allentoft, M.E., Armit, I., Kristiansen, K., Booth, T., Reich, D., 2018. The Beaker phenomenon and the genomic transformation of northwest Europe. Nature 555, 190–196.
O'Sullivan, N., Posth, C., Coia, V., Schuenemann, V.J., Price, T.D., Wahl, J., Maixner, F., 2018. Ancient genome-wide analyses infer kinship structure in an Early Medieval Alemannic graveyard. Sci. Adv. 4 (9), eaao1262.
Pashkova, V., 1963. Essays of the forensic-medical osteology: determination of gender, age and height by the bones of skeleton. State Press of Medical Literature, Moscow (in Russian).
Patterson, N., Price, A.L., Reich, D., 2006. Population structure and eigenanalysis. PLoS Genet. 2 (12), e190.
Patterson, N., Moorjani, P., Luo, Y., Mallick, S., Rohland, N., Zhan, Y., Reich, D., 2012. Ancient admixture in human history. Genetics 192 (3), 1065–1093.
Petr, M., Vernot, B., Kelso, J., 2019. admixr—R package for reproducible analyses using ADMIXTOOLS. Bioinformatics 35 (17), 3194–3195.
Petrosyan, L., 2022. Das Gräberfeld Von Lchashen Am Sevan-See (armenien), Veröffentlichungen Des Landesamtes Für Denkmalpflege Und Archäologie Sachsen-Anhalt – Landesmuseum Für Vorgeschichte, Bd. 89. Landesmuseum für Vorgeschichte, Halle.
Petrosyan, L.A., 2018. The necropolis of Lchashen. Archaeological Sites of Armenia 22, Institute of Archaeology and Ethnography Publishing, Yerevan (in Armenian).
Piggott, S., 1968. The earliest wheeled vehicles and the Caucasian evidence. Proceedings of Prehistoric Society 34, 266–318.
Pinhasi, R., Fernandes, D., Sirak, K., Novak, M., Connell, S., Alpaslan-Roodenberg, S., Hofreiter, M., 2015. Optimal Ancient DNA Yields from the Inner Ear Part of the Human Petrous Bone. PLoS One 10 (6), e0129102.
Purcell, S., Neale, B., Todd-Brown, K., Thomas, L., Ferreira, M.A.R., Bender, D., Maller, J., de Bakker, P.I.W., Daly, M.J., Sham, P.C., 2007. PLINK: a toolset for whole-genome association and population-based linkage analysis. Am. J. Hum. Genet. 81 (3), 559–575.
Ramstetter, M.D., Shenoy, S.A., Dyer, T.D., Lehman, D.M., Curran, J.E., Duggirala, R., Blangero, J., Mezey, J.G., Williams, A.L., 2018. Inferring identical-by-descent sharing of sample ancestors promotes high-resolution relative detection. Am J Hum Genet. 103 (1), 30–44. https://doi.org/10.1016/j.ajhg.2018.05.008.
Reimer, P.J., et al., 2020. The IntCal20 Northern Hemisphere Radiocarbon Age Calibration Curve (0–55 cal kBP). Radiocarbon 62, 725–757.
Rohland, N., Reich, D., 2012. Cost-effective, high-throughput DNA sequencing libraries for multiplexed target capture. Genome Res. 22 (5), 939–946.
Rubinacci, S., Ribeiro, D.M., Hofmeister, R.J., et al., 2021. Efficient phasing and imputation of low-coverage sequencing data using large reference panels. Nat Genet 53, 120–126. https://doi.org/10.1038/s41588-020-00756-0.
Schroeder, H., Margaryan, A., Szmyt, M., Theulot, B., Włodarczak, P., Rasmussen, S., Gopalakrishnan, S., Szczepanek, A., Konopka, T., Jensen, T.Z.T., Witkowska, B., Wilk, S., Przybyła, M.M., Pospieszny, Ł., Sjögren, K.G., Belka, Z., Olsen, J., Kristiansen, K., Willerslev, E., Frei, K.M., Sikora, M., Johannsen, N.N., Allentoft, M. E., 2019. Unraveling ancestry, kinship, and violence in a Late Neolithic mass grave. Proc Natl Acad Sci U S A. 116 (22), 10705–10710. https://doi.org/10.1073/pnas.1820210116.
Schubert, M., Ginolhac, A., Lindgreen, S., Thompson, J.F., Al-Rasheid, K.A.S., Willerslev, E., Orlando, L., 2012. Improving ancient DNA read mapping against modern reference genomes. BMC Genomics 13, 178.
Schubert, M., Ermini, L., Der Sarkissian, C., Jónsson, H., Ginolhac, A., Schaefer, R., Orlando, L., 2014. Characterization of ancient and modern genomes by SNP detection and phylogenomic and metagenomic analysis using PALEOMIX. Nat. Protoc. 9 (5), 1056–1082.
Schubert, M., Lindgreen, S., Orlando, L., 2016. AdapterRemoval v2: rapid adapter trimming, identification, and read merging. BMC. Res. Notes 9, 88.
Schwarz, R., 2014. Goldene Schläfen- und Lockenringe: Herrschaftsinsignien in Bronzezeitlichen Ranggesellschaften Mitteldeutschlands: Überlegungen zur Gesellschaft der Aunjetitzer Kultur. In: Meller, H., Risch, R., Pernicka, E. (Eds.), Metalle Der Macht - Frühes Gold Und Silber. Landesamt für Denkmalpflege und Archäologie in Sachsen-Anhalt, Landesmuseum für Vorgeschichte, Halle (Saale), pp. 717–742.
Sikora, M., Pitulko, V.V., Sousa, V.C., Allentoft, M.E., Vinner, L., Rasmussen, S., Willerslev, E., 2019. The population history of northeastern Siberia since the Pleistocene. Nature 570 (7760), 182–188.
Skoglund, P., Storå, J., Götherström, A., Jakobsson, M., 2013. Accurate sex identification of ancient human remains using DNA shotgun sequencing. J. Archaeol. Sci. 40 (12), 4477–4482.
Skoglund, P., Thompson, J.C., Prendergast, M.E., Mittnik, A., Sirak, K., Hajdinjak, M., Reich, D., 2017. Reconstructing prehistoric African population structure. Cell 171 (1), 59–71.e21.
Sousa da Mota, B., Rubinacci, S., Cruz Dávalos, D.I., et al., 2023. Imputation of ancient human genomes. Nat Commun 14, 3660. https://doi.org/10.1038/s41467-023-39202-0.
Storaci, M., Gilibert, M., 2019. Les poissons muets. Fish shaped vishaps and cult of water in prehistoric Armenia. In: Bobokhyan, A., Gilibert, A., Hnila, P. (Eds.), Vishap

between Fairy Tale and Reality. Institute of Archaeology and Ethnography Publishing, Yerevan, pp. 528–545.
Teschler-Nicola, M., et al., 2020. Ancient DNA reveals monozygotic newborn twins from the Upper Palaeolithic. https://www.nature.com/articles/s42003-020-01372-8.
Vågene, Å.J., Herbig, A., Campana, M.G., et al., 2018. Salmonella enterica genomes from victims of a major sixteenth-century epidemic in Mexico. Nat Ecol Evol 2, 520–528. https://doi.org/10.1038/s41559-017-0446-6.
Valdiosera, C., Günther, T., Vera-Rodríguez, J.C., Ureña, I., Iriarte, E., Rodríguez-Varela, R., … Jakobsson, M., 2018. Four millennia of Iberian biomolecular prehistory illustrate the impact of prehistoric migrations at the far end of Eurasia. Proceedings of the National Academy of Sciences of the United States of America 115(13), 3428–3433.
Vardanyan, B.V., 2019. Issues of Sociodemographic Differentiation for the Late Bronze Age in the Territory of Kura-Araxes Interfluve according to the Lchashen Necropolis (16 –13th cc. BC). In: Dalalyan, T., Hovsepyan, R., Babajanyan, A. (Eds.). Proceedings of the Institute of Archaeology and Ethnography 3. Institute of Archaeology and Ethnography Publishing, Yerevan, pp. 65-78 (in Armenian).
Vogel, J.S., Southon, J.R., Nelson, D.E., Brown, T.A., 1984. Performance of catalytically condensed carbon for use in accelerator mass spectrometry. Nucl. Instrum. Methods Phys. Res., Sect. B 5 (2), 289–293.
Wang, C.-C., Reinhold, S., Kalmykov, A., Wissgott, A., Brandt, G., Jeong, C., Haak, W., 2019. Ancient human genome-wide data from a 3000-year interval in the Caucasus corresponds with eco-geographic regions. Nat. Commun. 10 (1), 590.
Waples, R.K., Albrechtsen, A., Moltke, I., 2019. Allele frequency-free inference of close familial relationships from genotypes or low-depth sequencing data. Mol. Ecol. 28 (1), 35–48.
Weissensteiner, H., Pacher, D., Kloss-Brandstätter, A., Forer, L., Specht, G., Bandelt, H.-J., Schönherr, S., 2016. HaploGrep 2: mitochondrial haplogroup classification in the era of high-throughput sequencing. Nucleic Acids Res. 44 (W1), W58–W63.
Zaharia, E., 1959. Die Lockenringe von Sărata Monteoru und ihre typologischen und chronologischen Beziehungen. Dacia, n.s. 3, 103–134.
Zakaryan, E., 2014. Reflections of twin-myths in Armenian fairy-tales. Voske Divan: Journal of Fairy-Tale Studies 5, 66–77 in Armenian.
Zimmer, K., 2019. Los esqueletos de la península ibérica cuentan su historia genética. The New York Times, 19 March. https://www.nytimes.com/es/2019/03/19/adn-historia-peninsula-iberica/.